

Regulation of microtubule array in its self-organized dense active crowds

Xin-Chen Jiang(蒋新晨), Yu-Qiang Ma(马余强), Xiaqing Shi(施夏清)

Citation: Chin. Phys. B . 2020, 29(7): 078201 . **doi:** 10.1088/1674-1056/ab9430
Journal homepage: http://cpb.iphy.ac.cn; http://iopscience.iop.org/cpb

What follows is a list of articles you may be interested in

Quartic coupling and its effect on wetting behaviors in nematic liquid crystals

Zeng Ming-Ying, Holger Merlitz, Wu Chen-Xu

Chin. Phys. B . 2015, 24(2): 026101 . **doi:** 10.1088/1674-1056/24/2/026101

Dynamic aggregation evolution of competitive societies of cooperative and noncooperative agents

Lin Zhen-Quan, Ye Gao-Xiang

Chin. Phys. B . 2013, 22(5): 058201 . **doi:** 10.1088/1674-1056/22/5/058201

Kinetic evolutionary behavior of catalysis-select migration

Wu Yuan-Gang, Lin Zhen-Quan, Ke Jian-Hong

Chin. Phys. B . 2012, 21(6): 068201 . **doi:** 10.1088/1674-1056/21/6/068201

Azimuthal anchoring of a nematic liquid crystal on a grooved interface with anisotropic polar anchoring

Zhou Xuan, Zhang Zhi-Dong, Ye Wen-Jiang, Xuan Li

Chin. Phys. B . 2012, 21(6): 066104 . **doi:** 10.1088/1674-1056/21/6/066104

SPECIAL TOPIC — Active matters physics

Regulation of microtubule array in its self-organized dense active crowds*

Xin-Chen Jiang(蒋新晨)[1], Yu-Qiang Ma(马余强)[2,†], and Xiaqing Shi(施夏清)[1,‡]

[1] Center for Soft Condensed Matter Physics and Interdisciplinary Research, & School of Physical Science and Technology, Soochow University, Suzhou 215006, China

[2] National Laboratory of Solid State Microstructures and Department of Physics, Nanjing University, Nanjing 210093, China

(Received 19 April 2020; revised manuscript received 12 May 2020; accepted manuscript online 19 May 2020)

Microtubule self-organization under mechanical and chemical regulations plays a central role in cytokinesis and cellular transportations. In plant-cells, the patterns or phases of cortical microtubules organizations are the direct indicators of cell-phases. The dense nematic pattern of cortical microtubule array relies on the regulation of single microtubule dynamics with mechanical coupling to steric interaction among the self-organized microtubule crowds. Building upon previous minimal models, we investigate the effective microtubule width, microtubule catastrophe rate, and zippering angle as factors that regulate the self-organization of the dense nematic phase. We find that by incorporating the effective microtubule width, the transition from isotropic to the highly ordered nematic phase ($N_{\rm I}$ phase) with extremely long microtubules will be gapped by another nematic phase which consists of relative short microtubules ($N_{\rm II}$ phase). The $N_{\rm II}$ phase in the gap grows wider with the increase of the microtubule width. We further illustrate that in the dense phase, the collision-induced catastrophe rate and an optimal zippering angle play an important role in controlling the order–disorder transition, as a result of the coupling between the collision events and ordering. Our study shows that the transition to dense microtubule array requires the cross-talk between single microtubule growth and mechanical interactions among microtubules in the active crowds.

Keywords: microtubule array, nematic order, zippering, microtubule growth

PACS: 82.20.−w, 61.30.Hn, 02.70.Uu **DOI:** 10.1088/1674-1056/ab9430

1. Introduction

Dense ordered cortical microtubule (CMT) arrays is widely found in the interphase of plant cell.[1–3] The array structure is known to further dictate the direction of cell expansion. It plays a key role in consequent plant cell morphogenesis.[4–7] To understand the self-organization principle, *in vivo* fluorescent image reveals significant microtubule interaction during the polymerization process.[8–12] It has been shown that the steric interaction between microtubules will lead to zippering into microtubule bundles if they encounter each other at shallow angle. If they encounter each other at large angle, the blocked microtubules may stop growing, or crossover by protruding to the third dimension, and in some cases even induce dynamic catastrophe triggering fast depolymerization.[10,11] These dynamic processes are shown to be critical in leading to the formation of ordered dense microtubule array.[11,13–15] Furthermore, more and more microtubule associated proteins have been identified to reveal how these ordered microtubule arrays might respond to the external mechanical, geometrical, and chemical signals.[8,12,16–24]

These experimental findings inspire intensive studies on the self-organization of the microtubule array both numerically and theoretically, which leads to a general physical picture of 'survival-of-the-aligned' mechanism.[13–15,25–30] In these models,[14,25] microtubules are attached to cell cortical membrane in 2D and undergo polymerization and elongation during the formation of interphase microtubule array. Frequent collisions, zippering, and catastrophe events finally punish those discordant microtubles, and let the concordant ones survive long enough to self-organize into an ordered state.[30]

Detailed calculations provide a basic understanding of the order–disorder transition and the governing process.[14,15] Computer simulation thus turns out to be an efficient tool not only to illustrate the underlying ordering mechanism, but also for the illustration of possible rules guiding the organization process with the assistance of microtubule associated proteins.[14,15,18,21,25–27,30–35] For the simplest situation, it has been shown that simple mechanical-growth coupling is enough for the formation of ordered microtubule array. The regulation of cortical microtubule nucleation/polymerization/depolisymerizaiton is essential for the order–disorder transition in such system. In simulations, the role of microtubule associated proteins, such as katanin, etc., can also been taken into account.[17,30,31] Detailed dynamic regulations can be well captured by computer simulations and studied in a systematic way. Interesting factors like the topology of the cell compartment and 3D geometries can also be

*Project supported by the National Natural Science Foundation of China (Grant Nos. 11474155, 11774147, 11674236, and 11922506).

†Corresponding author. E-mail: myqiang@nju.edu.cn

‡Corresponding author. E-mail: xqshi@suda.edu.cn

© 2020 Chinese Physical Society and IOP Publishing Ltd

taken into account,[18,24,34] which further reveals the importance of mechanical constraints on the regulation of microtubule array morphology.

In this paper, following the spirit of previous minimal model, we use computer simulations to study the possible effects of surface crowdedness on the self-organization of microtubule array in 2D. Microtubules are closely attached to the plant cell membrane, where various cellular activities and regulations take place.[1,2,6] *In vivo*, in such crowded condition, the decoration of microtubule associated proteins, motors, and cell membrane substrate, and even the screened electrostatic interaction might change the effective width of the microtubule and their inter spacing.[36–45] Previous models also show that without the inclusion of microtubule width, the microtubules may self-organize into a dense ordered array.[14,15,30] To address the effect of crowdedness, we have to take into account of the effective width of microtubules. We find that by introducing such an intrinsic geometry property, it can qualitatively change the phase behavior of the system. The additional crowdedness delays the order–disorder transition, and leads to an intermediate phase, which has only been observed in the very dense regime in a model with zero width.[15] The inclusion of microtubule width may further change the consequent collision relevant events, such as collision induced catastrophe and zippering.[11] These mechanical-growth couplings are incorporated in simulation to reveal how the plant cell might be able to regulate the mechanical response with optimal critical zippering angles.

2. Results and discussion

2.1. Event driven chemical kinetics with steric coupling

Here we model microtubules with a finite width in order to properly account for the exclude volume interaction in the dense phases of cortical microtubule array. With high growth rate, a line segment model with zero width may lead to ultra-high density. The effective width of microtubule thus plays an important role to regulate microtubule density in such phases. A schematic illustration of the model is shown in Fig. 1. The basic building blocks of the model are rectangles with varying length $l_{j,k}$ and width W, where the subscripts denote the k^{th} segment on j^{th} microtubule in the system. The very ends of micotubules are covered with semicircles with radius $R = W/2$. The interaction between microtubules is the hard rod potential, and any overlap of microtubules is strictly forbidden in the model. The growth of a microtubule is blocked if there is no non-overlapping space near the plus end. The nucleation of new microtubule can happen only in place where free-space for new microtubule with segment length Δl plus the circular caps is available.

Following previous studies, at present coarse-grained level, the single microtubule dynamics are sufficiently described by the growth/catastrophe/shrinkage/rescue on the plus end of the microtubule and shrinkage on the minus end.[25,46,47] The growth speed k_{g} on the plus end is usually larger than the shrink speed k_{sm} on the minus end, otherwise the microtubule cannot exist for long time. The catastrophe rates on the plus end can be distinguished by spontaneous catastrophe rate k_{sc} and collision induced catastrophe rate k_{ic}. In the dilute limit, since collisions among microtubules are rare, we can expect that spontaneous catastrophe is more dominant than induced catastrophe.[48,49] But here, since we are interested in the dense phase, collision happens so frequently that the induced catastrophe may dominate the catastrophe events.[50] The catastrophe events will lead to the shrinkage of microtubule k_{s} on the plus end. Microtubules can resume growth with a rescue rate k_{r}. The typical values of the kinetic parameters used in the simulations are listed in Table 1.

Table 1. List of parameters and values in the simulation.

	Parameters	Simulated values
k_{g}	plus-end polymerization rate	40–80 nm/s
k_{s}	plus-end depolymerization rate	160 nm/s
k_{sm}	minus-end depolymerization rate	40 nm/s
k_{r}	rescue rate	0.01/s
k_{sc}	spontaneous catastrophe rate	0.00–0.02 s^{-1}
k_{ic}	induced catastrophe rate	0.00–0.14 s^{-1}
k_{n}	nucleation rate rate	3 $\mu\text{m}^{-2}\cdot\text{s}^{-1}$
α_0	critical zippering angle	0°–90°
α_{c}	critical angle for collision induced catastrophe	$\sim 40°$
Δl	subunit length	10 nm
L	system size	8 μm
T	total simulation time	$\sim 10^6$ s
W	effective width	0–50 nm

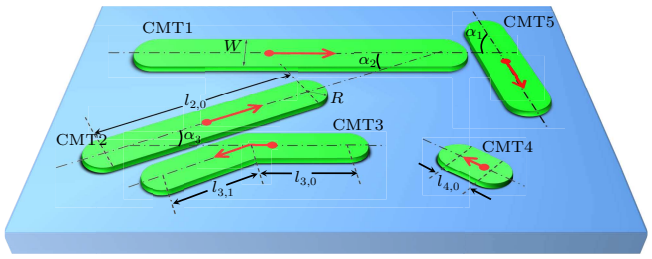


Fig. 1. Schematic representation of an interacting kinetic growth model for microtubules with finite width W. The size of an individual microtubule j is described by a constant width W, and segment lengths $l_{j,k}$, where the subscripts denote the k^{th} segment on j^{th} microtubule in the system. Every microtubule is covered with semicircle at both ends. The dash-dotted line indicates the central axis of microtubule, and the red arrow indicates the plus-end direction. In the cartoon, CMT2 will collide with CMT1 by further polymerization. α_j is the colliding angle of the j^{th} microtubule with its neighbor. The result depends on the choice of an critical zippering angle α_0. For steep angle with $\alpha_j > \alpha_0$, the growth of microtubule is blocked and may trigger induced catastrophe; for shallow angle $\alpha_j < \alpha_0$, such as CMT3, it will zipper and grow along its colliding neighbor's body axis. CMT4 represents a newly nucleated one in the free space.

During the growth, the microtubules may encounter each other. The growth of blocked microtubule will be stopped since no free space is available for the addition of a new segment. Microtubules are quite rigid, with typical persistence

length of several millimeters.[51] The small flexibility still allows it to deviate its original growth direction. In experiment, the so called zippering events are observed when two microtubules encounter, or even crossover if microtubule growth into the third dimension out of the plane.[11,50] For simplicity, here we restrict ourselves to strictly 2D, thus we do not consider the crossover events. For zippering, it has been observed that such event depends on the relative angle α between colliding microtubules.[11,52] We can define a critical α_0 to approximate the angular dependence. If the collision angle $\alpha > \alpha_0$, zippering is not possible. If the system allows induced catastrophe, then such large angle encounter would trigger such event with a rate $k_{\rm ic}$. For $\alpha < \alpha_0$, zippering will take place, and the colliding microtubule changes its growth orientation following the direction dictated by the encountered microtubule (see Fig. 1).

We apply the event driven Gillespie algorithm to simulate our mechanical–chemical coupled dynamic system.[29–31,53] In each simulation step, the time is forwarded according to $\delta t = a_0^{-1}\ln(1/r)$, where $r \in (0,1]$ is a uniform random number and $a_0 = k_{\rm n}L^2 + (k_{\rm g}N_+ + k_{\rm s}N_- + k_{\rm sm}N)/\Delta l + k_{\rm r}N_- + k_{\rm sc}N_+ + k_{\rm ic}N_{\rm b}$ is the sum of rates of all possible events. Here, N_+ and N_- are the numbers of microtubules in the growth-state and shrink-state on the plus-end, respectively, and Δl is the length of a discrete segment we add onto the microtubule. $N_{\rm b}$ is the number of microtubules which are blocked by encountering microtubules with the relative angle $\alpha > \alpha_{\rm c}$, and the corresponding term is responsible for the induced catastrophe. $\alpha_{\rm c}$ is the critical angle for collision induced catastrophe. Notice here that the term responsible for spontaneous catastrophe is $k_{\rm sc}N_+$, while for induced catastrophe is $k_{\rm ic}N_{\rm b}$. $N_{\rm b}$ is the number of blocked configurations for microtubules, and in all simulation we have $N_{\rm b} \le N_+$. In each simulation step, the algorithm will choose the stochastic event according to their relative weight. Once the algorithm decides a specific type of events (growth, shrinkage, nucleations, catastrophe, or rescue), it then randomly selects a specific microtubule with equal probability to realize such event. For growth and nucleation events, if we find the added segment with Δl overlap with the existing microtubule, we skip the growth/nucleation, keep the original configuration, and let the time increase. This leaves a gap at the tip of the blocked microtubule, which is a natural outcome of discretized nature of the segment.

The order of the system can be measured according the magnitude of weighted nematic order parameter tensor as defined in Refs. [15,30], which is given by

$$S = \left\langle \frac{\sqrt{(\sum_{j,k} l_{j,k}\sin 2\theta_{j,k})^2 + (\sum_{j,k} l_{j,k}\cos 2\theta_{j,k})}}{\sum_{j,k} l_{j,k}} \right\rangle, \quad (1)$$

where $\langle\cdots\rangle$ represents time average, $l_{j,k}$ and $\theta_{j,k}$ are the length and orientation of the $j^{\rm th}$ microtubule's $k^{\rm th}$ straight segment, respectively, and the summation is over all the segments in the system. The system is in disorder state if the measured S in simulation is close to zero, here we choose $S < 0.3$ for finite system sizes simulated here. $S = 1$ is the state that all microtubules completely align. By default, all the simulations are started from empty states unless specified.

To see how the collective behavior of the dense microtubule array may be affected by the effective microtubule width and other dynamic processes, in the following sections we first use a simple tread milling model where the critical angle α_0 for zippering is set to 0°, and neglect catastrophe events on the plus-end of the microtubule. Next, we switch on the spontaneous and induced catastrophe events and demonstrate their relative importance in controlling the order–disorder transition. Finally, we vary the critical zippering angle α_0 and show the optimal regime to achieve nematic order.

2.2. Cortical microtubule self-organization with effective microtubule width

To simulate crowded cortical microtubule array, we have to take into account of the effective width of single microtubule in the model. *In vivo*, the effective width of microtubule may differ from that of bare microtubule due to the complicated cortical environment and electrostatic interactions. First microtubules are strongly attached to the cell membrane, thus the membrane and associated proteins may mediate the effective interaction among microtubules. Moreover, the decoration of microtubule associated proteins may also change the effective width directly. In Fig. 2, we show how the effective width may change the order–disorder transition in the model

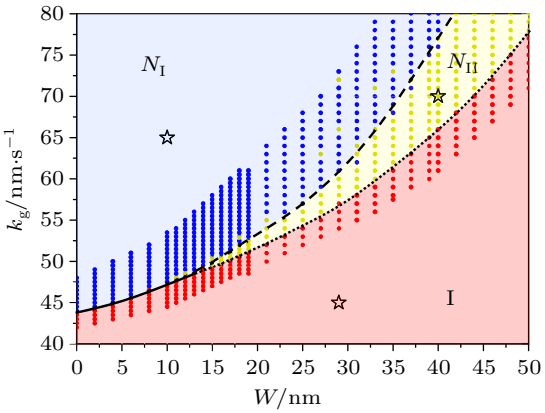


Fig. 2. Phase diagram by changing ($k_{\rm g}$, W) parameters. Three phases are indicated, disorder isotropic phase (I) (pink region), nematic I phase with highly aligned and very long microtubules ($N_{\rm I}$) (blue region), and nematic II phase with relative short aligned microtubules ($N_{\rm II}$) (yellow region). Solid dots are samples for which simulations are performed. The star symbols represent the typical cases used in the analysis in Fig. 3, for I phase ($W = 28$ nm, $k_{\rm g} = 45$ nm/s) (see ESI-Movie1.mov), $N_{\rm I}$ phase ($W = 10$ nm, $k_{\rm g} = 65$ nm/s) (see ESI-Movie2.mov), and $N_{\rm II}$ phase ($W = 40$ nm, $k_{\rm g} = 70$ nm/s) (see ESI-Movie3.mov), respectively. Here the critical zippering angle $\alpha_0 = 0$. The spontaneous catastrophe and collision induced catastrophe are not taken into account in this phase diagram. Other parameters are given in Table 1. For every data point we performed one single thread simulation with time 10^5–5×10^5 s.

system. In the phase diagram of Fig. 2, with the increase of the effective width W, the second nematic state emerges. Following previous studies, we denote the highly ordered nematic state with very long microtubules as $N_{\rm I}$ and relatively lowly ordered nematic state with short microtubules as $N_{\rm II}$ (see Figs. 3(a) and 3(b)). These properties have been well captured by the angular and length probability density function (PDF) of microtubules. As shown in Fig. 3(a), the angular distribution of the $N_{\rm I}$ phase is in a narrow range of angle around the super sharp peak, while the $N_{\rm II}$ phase although also has a dominant angle, indicating the emergence of nematic order, its distribution is broad. The length distribution also shows the singularity behavior of the $N_{\rm I}$ phase. The system shows a very broad length distribution until several thousand microns. The disorder phase and $N_{\rm II}$ phase, on the other hand, both show clear exponential decay of microtubule length.

Although the symmetry of the $N_{\rm II}$ and $N_{\rm I}$ phases is the same, the transition between these two phases is usually discontinuous (first order-like), thus they could be well

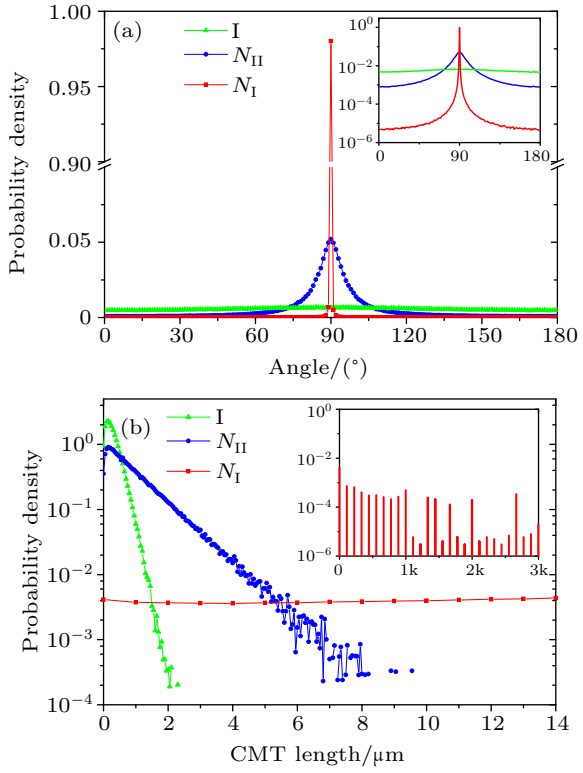


Fig. 3. Microtubule angular and length PDF for three typical cases as indicated by the star symbols in Fig. 2. (a) Angular PDF counted by subunits for three typical cases in three different phases. Isotropic phase I in green, sharply aligned $N_{\rm I}$ phase in red, and aligned microtubules with broad angular distribution $N_{\rm II}$ phase in blue. The distribution is obtained by time average of samples. Each sample is rotated with its dominant distribution at 90°. The vertical axis breaks at 0.1–0.9 to show the sharp red peak clearer ($N_{\rm I}$ phase) which is about 20 times higher than the blue peak ($N_{\rm II}$ phase). Inset: the vertical axis in log scale. (b) Length probability PDF of number of microtubules. Both isotropic (green) and $N_{\rm II}$ (blue) phases demonstrate exponential decay in the length distributions. The $N_{\rm I}$ phase shows a very broad length distribution, which indicates that the system is dominated by extremely long microtubules. The analysis is performed in the steady state for a period 2×10^5 s with an interval of 10^3 s. Inset: microtubule length distribution in $N_{\rm I}$ phase with much broader range of length.

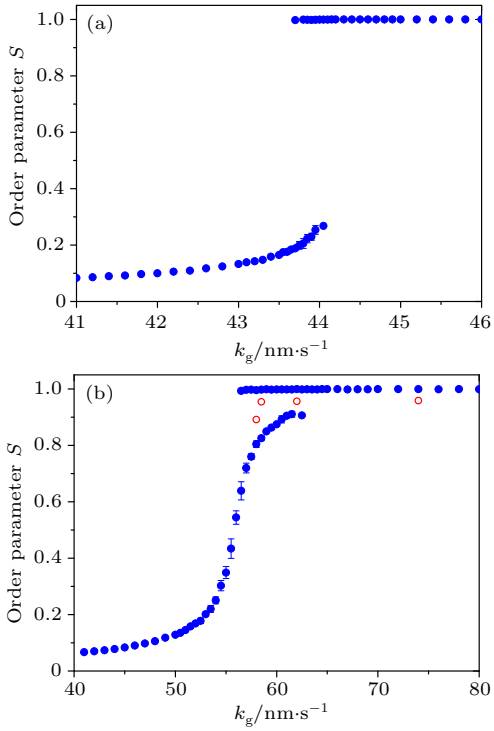


Fig. 4. Isotropic nematic transitions for different effective microtubule widths. (a) Almost direct transition from disorder I phase to nematic $N_{\rm I}$ phase for $W = 0$ nm with the increase of growth rate $k_{\rm g}$. The transition is discontinuous characterized by the coexistence regime near $k_{\rm g} = 44$ nm/s. (b) For $W = 25$ nm, the transition from disorder I phase to $N_{\rm II}$ phase, then jumping into $N_{\rm I}$ phase with the increase of growth rate $k_{\rm g}$. The $N_{\rm II}$ and $N_{\rm I}$ phase transition is discontinuous, with a bistable regime near $k_{\rm g} = 60$ nm/s. The order parameter S is obtained by time and sample average (20 samples). Errors bar for 20 independent samples are given and most are within the symbol. Red circles represent that simulation samples undergo phase transition process and do not reach the steady state within the simulation time $\sim 5\times10^5$ s, giving the strong discontinuous nature of the transition, which is not included for averaging. Other parameters not listed here are the same as those in Fig. 2.

distinguished by studying how order parameter S varies with the control parameters. Here, we choose to fix the effective width $W = 0$ nm and $W = 25$ nm and increase the polymerization rate $k_{\rm g}$ so that we can expect a direct transition from isotropic phase I to $N_{\rm I}$ phase at $W = 0$ nm, and an intermediate transition into $N_{\rm II}$ phase at $W = 25$ nm. We measure order parameter S as defined in Eq. (1). As shown in Fig. 4(a), for $W = 0$ nm, the transition between isotropic phase and $N_{\rm I}$ phase is discontinuous, characterized by a coexistence regime around $k_{\rm g} = 44$ nm/s. The discontinuity is a result of mutual enhancement of nematic order and increasing microtubule length. Without effective width, the transition can happen at relative low growth rate, with a direct jump between disorder and ordered states. For $W = 25$ nm, as shown in Fig. 4(b) the effect of crowdedness of the system is shown to change the transition from disorder to $N_{\rm I}$ phase. Although there still exist the mutual enhancement microtubule length and nematic order, the growth of microtubule is much easily blocked by other microtubules. With the increase of W, the microtubule occupied area will dramatically block the growth. Such strong steric effects thus delay the order–disorder transition, and can

constrain the length distribution to be exponential even when the system becomes nematic ordered. As a result, the system can continuously go into the nematic N_{II} phase until very large polymerization rate, as shown in Fig. 4(b). When the order parameter S gets larger, the system finally breaks the blockage and dramatically elongates the microtubules with the formation of N_I phase. The large coexistence regime of N_{II} and N_I phases near $k_g = 60$ nm/s clearly indicates the discontinuity of such process.

As a result, in the phase diagram of Fig. 2, the border between N_I and N_{II}/I phases is first order-like (discontinuous), and the border between I and N_{II} phases is second order-like (continuous). The interception point of these two transition lines is the so called tricritical point. A similar topology of the phase diagram also exists in a model without the inclusion of the effective microtubule width.[15] In such case, the N_{II} phase will emerge if the system has a very large nucleation rate to produce lots of short microtubules in the model with $W = 0$ nm. Here, we have kept the nucleation rates unchanged, even effectively reduced with an effective width, but the inclusion of effect width increases the crowdedness of the system without further sharpening of the order. This plays the similar role as the nucleation of short disorder microtubules in previous model.

2.3. Spontaneous and induced catastrophes in dense phase

With the inclusion of the effective width, we now check how the catastrophe events will be coupled to the finite width microtubule system. The collision induced catastrophe depends on the blocked configurations among growing microtubules. In the dilute limit of the microtubule system, with negligible collisions, the spontaneous catastrophe plays much important roles. It regulates the length distribution and thus also the order property of the system. In the dense phase, the induced catastrophe becomes much important due to the frequent collisions among microtubules. We are interested here to see how different catastrophes may effect the self-organization of the dense phase.

For this purpose, we choose $W = 25$ nm (approximately the bare width of microtubule) and $k_g = 70$ nm/s with rescue rate $k_r = 0.01$ s^{-1} (see Table 1), where the system stays in N_I phase without introducing catastrophe. To compare the difference of two catastrophe mechanisms, we focus on two cases where spontaneous catastrophe and induced catastrophe are introduced separately. As shown in Fig. 5(a), both catastrophe events can drive the system decay from N_I to N_{II} and then disorder. The catastrophes trigger the depolymerization process k_s on the plus-end, and the microtubule thus will shrink on both ends, and the length is shortened efficiently. This will reduce the microtubule length and lead to less ordered state. The transition from N_I to N_{II} is still discontinuous (first order-like), and N_{II} to isotropic is continuous (second order-like). The transition from N_I phase to N_{II} is more sensitive to spontaneous catastrophe k_{sc}. In N_I phase, the system is extremely crowded, however, the microtubules are highly aligned. Perfect alignment dramatically reduces the collisions among microtubules, which makes the transition less sensitive to induced catastrophe rate k_{ic}.

Since k_{ic} needs the collision process to trigger the catastrophe, its value does not represent the frequency of catastrophe events that actually take place in the system. We can further compare the effects of both catastrophes by the frequency of real catastrophe events (RCEs). We count the average frequency of RCEs in simulations for both cases in steady state. The statistics are shown in Fig. 5(b).

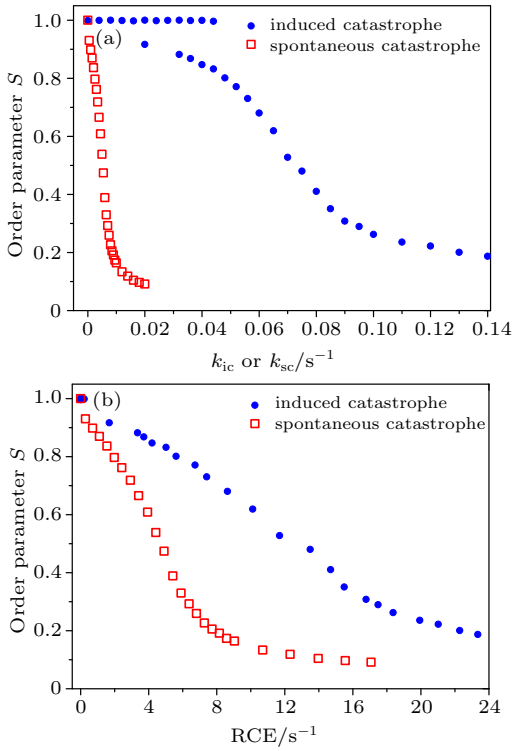


Fig. 5. Spontaneous catastrophe and induced catastrophe in regulation of order–disorder transition. (a) The transition from N_I phase to less ordered N_{II} phase and disorder with the increase of spontaneous catastrophe rate k_{sc} (red square) or k_{ic} (blue dot). (b) Same data as (a) but the horizontal-axis is mapped to the time averaged frequency of real catastrophe events (RCE) for all the samples. The critical angle for collision induced dynamic catastrophe is $\alpha_c = 40°$, the growth speed $k_g = 70$ nm/s, and effective microtubule width $W = 25$ nm. The simulations start from N_I state as obtained in Fig. 4(b) at $k_g = 70$ nm/s. Each point is averaged with 5 samples with time interval 1 s, and average simulation time longer than 10^5 s.

There are two important features in such representation. First, compared with Fig. 5(a), the significant overlap of N_{II} and N_I phases for induced catastrophe disappears. It signifies that the N_{II} and N_I phases have very different RCEs even in the coexistence regime. For given k_{ic} in the coexistence regime in Fig. 5(a), the RCEs in highly ordered N_I phase are almost 0, while for relatively lowly ordered N_{II} phase, there exist quite significant collisions among microtubules, thus quite large RCEs are obtained.

Second, for given RCEs, the induced catastrophe still demonstrates significantly higher nematic order than the case for spontaneous catastrophe. The spontaneous catastrophe events only depend on the number of microtubules that are in the growth state, as we can see from the term $k_{sc}N_+$ in Eq. (1). However, the induce catastrophe events further require that these microtubules are blocked by neighbors ($k_{ic}N_b$ in Eq. (1)). Since micortubules that are not aligned with their neighbors are much easier to be blocked during the growth, collision induced catastrophes are much efficient to recognize and clean the discordant microtubules than spontaneous catastrophe, thus allowing larger nematic order at the same RCEs.

2.4. Optimal zippering angle

Zippering also depends on the collision among microtubules. In an active dense phase, we expect it would play an important role in controlling the order–disorder transition. One important parameter controling the zippering events is the critical angle α_0. When the colliding angle α is less than α_0, two microtubules will zipper. However, when colliding angle α is larger than α_0, we expect it is going to block the growth, and even can trigger collision induced catastrophe or crossover events. As we show above, catastrophe events basically are going to reduce the order in the system monotonously. Its effects can be compensated by increasing the growth speed. Here to investigate the effect of zippering, we set catastrophe to 0 s^{-1}. We also restrict ourselves strictly in 2D, thus do not consider the crossover events.

Zippering is considered a promotion effect of order in the system.[11] It helps to change dis-aligned microtubule groth along with their neighbor thus effectively introduces an alignment interaction. On the other hand, if zippering can happen very easily for large α, the microtubules essentially become very flexible. For flexible polymer, nematic order will disappear. To compromise the easiness of alignment and rigidity, we may expect an optimal critical zippering angle α_0 for nematic alignment.

In Fig. 6(a), we scan the (α_0, k_g) parameter space. It is clear that for large critical angle $\alpha_0 > 70^\circ$, the system becomes disorder even when k_g is large. For small α_0, at moderate growth rate 46 nm/s $< k_g <$ 55 nm/s, the system is also in a disordered state. The N_{II} phase exists only for an optimal α_0 region. Large α_0 drives the system into disorder. For small α_0, the N_I phase becomes dominant when k_g is large. In Fig. 6(b), these properties are further shown by an explicit plot of order parameter S versus α_0. In Fig. 6(a), we also notice that, near $k_g = 55$ nm/s, the reentrant behavior between N_I and N_{II} phases indicates that the zippering can modify the ordering in a non-trivial manner. In such condition for $\alpha_0 = 0^\circ$, the microtubules are always blocked during collision, and the system is locked in N_{II} phase. However, when a small α_0 is introduced, it allows the colliding microtubule to grow if the colliding angle $\alpha < \alpha_0$, and this suddenly drives the system into highly ordered N_I phase. Further increase of α_0 however makes the microtubules too flexible to maintain the N_I phase.

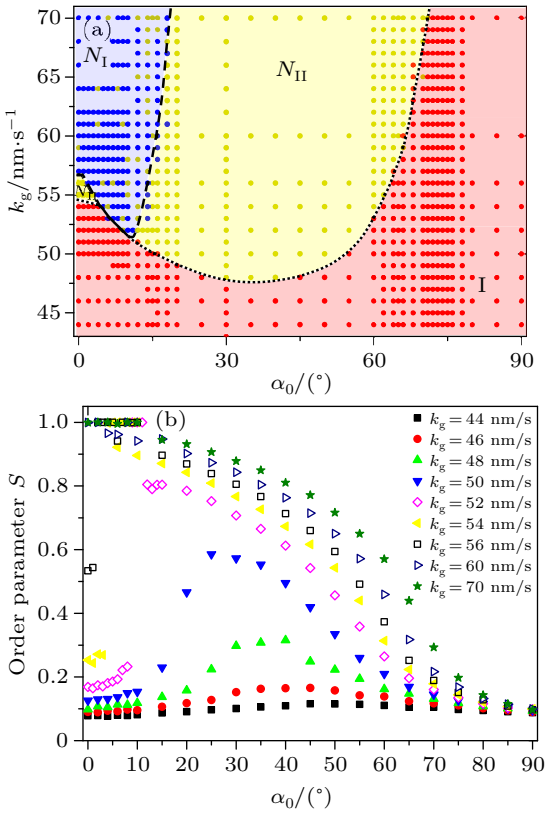


Fig. 6. The effects of critical zippering angle on growing microtubule phase behavior. (a) Phase diagram with the variations of critical zippering angle α_0 and k_g. The phase diagram is colored the same way as in Fig. 2. (b) The variations of time averaged order parameter S with the change of α_0 and k_g. The effective microtubule width used here is $W = 25$ nm, and $k_{ic} = k_{sc} = 0$ s^{-1}. The average is performed in the steady state with a sampling interval 1 s and total average period 10^5–5×10^5 s.

The optimal zippering angle indicates that zippering does not simply enhance the alignment. Although it enables the alignment of the growth direction of microtubules, it leaves those dis-aligned segments unchanged. Such dis-aligned segments can only be eliminated by depolymerization on the minus end. The catastrophe events on the plus-end would not help since it starts from the plus end and will eliminate the aligned part first. For large α_0, the zippering events happen irrespective of the colliding angle, which leads to frequent large angle bending of microtubules and drives the system into complete disorder.

In our simulation, by systematically varying the critical zippering angle α_0, we find optimal zippering angle around 30° to 40° for N_{II} phase. This optimal angle is consistent with the experimental determined zippering value. *In vivo*, various conditions may help regulating the critical angle for zippering. Since microtubules have large persistence length, the most important factor in control might be the microtubule associated proteins that fastens the microtubule on the cell cortex.[36,44,54]

Higher density of these binding proteins might allow small critical zippering angle. Moreover, the plus-end microtubule associated proteins might also play a role in the regulation of zippering. It would be interesting to investigate if evolution has allowed plant cell to exploit such possibility to do optimization for achieving ordered cortical microtubule array.

3. Conclusions

Through computer simulations, we incorporate the effects of effective width of cortical microtubule, the induced catastrophe events, and zippering effects to investigate the phase behavior in self-organized crowded microtubule array. We show that in the dense phase, the finite volume of microtubule plays an important role in regulating the order–disorder transition. It significantly enhances the probability of mutual blockage of microtubule growth, thus at finite density it is able to confine the growing microtubule length and suppresses the system into relatively lowly ordered $N_{\rm II}$ phase. With less free space it also triggers more collision induced catastrophe and zippering events, all these will further regulate the phase behavior of the microtubule array.

In the dense phase, we expect that the collisions among microtubules are frequent, thus the collision induced catastrophe and zippering of microtubules will become important. On the other hand, the dense phase usually corresponds to highly ordered nematic state.[55] The mutual alignment significantly reduces the collision process. These effects are revealed in our simulation, where we find in $N_{\rm I}$ phase the collision induced catastrophe rate is very low. Since the rate of collision induced catastrophe may change with the modification of local configuration, it will enhance the establishment of nematic order from a disordered state. First it will eliminate misaligned microtubules since these microtubules will trigger frequent catastrophe event if growing. Second, once microtubules are aligned, the induced catastrophe is dramatically reduced and locks the system in the ordered phase.

Our simulations show that the zippering mechanism is unexpectedly important in regulating the order formation in such dense microtubule array. Experimentally confirmed zippering critical angle is found to be optimal for the emergence of $N_{\rm II}$ phase. For small growth rate, both small and large zippering critical angles α_0 may lead to disorder. Our results suggest that the microtubule associated proteins that attach microtubules onto cell cortex will play an important role in regulating the critical zippering angle as observed *in vivo*.

References

[1] Ehrhardt D W and Shaw S L 2006 *Annu. Rev. Plant Biol.* **57** 859
[2] Paradez A, Wright A and Ehrhardt D W 2006 *Curr. Opin. Plant Biol.* **9** 571
[3] Elliott A and Shaw S L 2018 *Plant Physiol.* **176** 94
[4] Baskin T I 2005 *Annu. Rev. Cell Dev. Biol.* **21** 203
[5] Paredez A R, Somerville C R and Ehrhardt D W 2006 *Science* **312** 1491
[6] Bringmann M, *et al*. 2012 *Trends Plant Sci.* **17** 666
[7] Brandizzi F and Wasteneys G O 2013 *Plant J.* **75** 339
[8] Whittington A T, *et al*. 2001 *Nature* **411** 610
[9] Vos J W, Dogterom M and Emons A M C 2004 *Cell Motil. Cytoskeleton* **57** 246
[10] Shaw S L, Kamyar R and Ehrhardt D W 2003 *Science* **300** 1715
[11] Dixit R and Cyr R 2004 *Plant Cell* **16** 3274
[12] Murata T, *et al*. 2005 *Nat. Cell Biol.* **7** 961
[13] Baulin V A, Marques C M and Thalmann F 2007 *Biophys. Chem.* **128** 231
[14] Tindemans S H, Hawkins R J and Mulder B M 2010 *Phys. Rev. Lett.* **104** 058103
[15] Shi X Q and Ma Y Q 2010 *Proc. Natl. Acad. Sci. USA* **107** 11709
[16] Wasteneys G O 2002 *J. Cell Sci.* **115** 1345
[17] Nakamura M, Ehrhardt D W and Hashimoto T 2010 *Nat. Cell Biol.* **12** 1064
[18] Ambrose C, Allard J F, Cytrynbaum E N and Wasteneys G O 2011 *Nat. Commun.* **2** 1444
[19] Kirik A, Ehrhardt D W and Kirik V 2012 *Plant Cell* **24** 1158
[20] Shaw S L 2013 *Curr. Opin. Plant Biol.* **16** 693
[21] Lindeboom J J, *et al*. 2013 *Science* **342** 1245533
[22] Ambrose C and Wasteneys G O 2014 *Plant Cell Physiol.* **55** 1636
[23] Nakamura M 2015 *New Phytologist* **205** 1022
[24] Mirabet V, *et al*. 2018 *PLOS Comput. Biol.* **14** e1006011
[25] Hawkins R J, Tindemans S H and Mulder B M 2010 *Phys. Rev. E* **82** 011911
[26] Allard J F, Wasteneys G O and Cytrynbaum E N 2010 *Mol. Biol. Cell* **21** 278
[27] Eren E C, Dixit R and Gautam N 2010 *Mol. Biol. Cell* **21** 2674
[28] Deinum E E and Mulder B M 2013 *Curr. Opin. Plant Biol.* **16** 688
[29] Tindemans S H, Deinum E E, Lindeboom J J and Mulder B M 2014 *Front. Phys.* **2** 00019
[30] Deinum E E, Tindemans S H, Lindeboom J J and Mulder B M 2017 *Proc. Natl. Acad. Sci. USA* **114** 6942
[31] Deinum E E, Tindemans S H and Mulder B M 2011 *Phys. Biol.* **8** 056002
[32] Eren E C, Gautam N and Dixit R 2012 *Cytoskeleton* **69** 144
[33] Foteinopoulos P and Mulder B M 2014 *Bull. Math. Biol.* **76** 2907
[34] Chakrabortty B, Blilou I, Scheres B and Mulder B M 2018 *PLOS Comput. Biol.* **14** e1005959
[35] Eren E C, Dixit R and Gautam N 2015 *J. Math. Biol.* **71** 1353
[36] Sedbrook J C 2004 *Curr. Opin. Plant Biol.* **7** 632
[37] Hamada T 2014 *Int. Rev. Cell Mol. Biol.* **312** 1
[38] Minoura I and Muto E 2006 *Biophys. J.* **90** 3739
[39] Haselwandter C A and Wingreen N S 2014 *PLOS Comput. Biol.* **10** e1003932
[40] Schweitzer Y and Kozlov M M 2015 *PLOS Comput. Biol.* **11** e1004054
[41] Shi X Q and Ma Y Q 2007 *J. Chem. Phys.* **126** 125101
[42] Cantero M d R, Perez P L, Smoler M, Villa-Etchegoyen C and and Cantiello H F 2016 *Sci. Rep.* **6** 27143
[43] Santelices I B, *et al*. 2017 *Sci. Rep.* **7** 9594
[44] Oda Y 2018 *J. Plant Res.* **131** 5
[45] Barton D A, Vantard M and Overall R L 2008 *Plant Cell* **20** 982
[46] Dogterom M and Leibler S 1993 *Phys. Rev. Lett.* **70** 1347
[47] Howard J and Hyman A A 2003 *Nature* **422** 753
[48] Hamada T, Itoh T J, Hashimoto T, Shimmen T and Sonobe S 2009 *Plant Physiol.* **151** 1823
[49] Horio T and Murata T 2014 *Front. Plant Sci.* **5** 511
[50] Chi Z and Ambrose C 2016 *BMC Plant Biol.* **16** 18
[51] Gittes F 1993 *J. Cell Biol.* **120** 923
[52] Chan J, Sambade A, Calder G and Lloyd C 2009 *Plant Cell* **21** 2298
[53] Gillespie D T 1977 *J. Phys. Chem.* **81** 2340
[54] Liu Z, Persson S and Zhang Y 2015 *J. Integr. Plant Biol.* **57** 330
[55] Hitt L, Cross R and Williams C 1990 *J. Biol. Chem.* **265** 1639